Quantitative explanation of the observed population of Milky Way satellite galaxies

S. Koposov[1,4], J. Yoo[2], H.-W. Rix[1], D. Weinberg[3], A. Macciò[1], V. Belokurov[4]

[1]Max Planck Institute for Astronomy, Heidelberg, Germany [2]Harvard-Smithsonian Center for Astrophysics, Cambridge, USA

[3]Ohio State University, Department of Astronomy, Columbus, USA [4]Institute of Astronomy ,University of Cambridge, UK

Summary

We use the semi-analytical model of the Dark Matter halo/sub-halo evolution and several semi-analytical recipes for the star formation to simulate MW-like galaxy and its satellites and compare the number and the properties of dwarf galaxies in the simulations to the number and properties of observed dwarfs. The important ingredient in that comparison is the treatment of the incompleteness of existing observations (Koposov et al. 2007). We show that the models with the suppression of gas cooling after the epoch of re-ionization may reasonably well reproduce the observed number of dwarfs of different luminosities, the distribution of the velocity dispersions and the distance distributions.

DM Simulations

We performed the semi-analytical computation of the DM structure growth and accretion based on Press-Schechter merger trees which produce a MW-like DM halo at redshift of 0. That model traces the evolution of all the DM halos/sub-halos in such a way that we know their orbits, masses, sizes at all redshifts. The model also includes the effects of tidal stripping/destruction of the sub-halos orbiting around parent halos. The minimal MW sub-halo mass in the simulation has a mass ~10^5 Msun. In total we performed 6 Monte-Carlo realizations of the simulations to understand the influence of cosmic variance.

Star formation recipes

To compare the simulations with the observations we need to populate the DM halos with stars. In this work we tried several different simple recipes for the star formation in dwarf galaxies. The simplest one, which is known to be wrong: M_* M_{DM}

The simple modification of this recipe is the assumption that the stellar mass is proportional to the dark matter halo mass, but the star formation efficiency is a power-law function of the halo mass. $M_* = f_* M_{DM}$ where $f_* = f_{*,0} (M_{DM})^3$

The second, more realistic approach takes into account the re-ionization and the following stop of the star formation after it for small DM halos (following the Thoul&Weinberg 1996, Quinn&Katz 1996 results).

$$M_* = \begin{cases} f_* \times M_{DM} & \text{if } V_{circ}(z_{satellite}) > V_{crit} \\ f_* \times M_{DM}(z_{reion}) & \text{if } V_{circ}(z_{satellite}) < V_{crit} \end{cases}$$

In that model the stellar mass in the small DM halos is the stellar mass formed at the epoch of re-ionization and is proportional to the halo mass at that epoch, while large DM halos formed their stars mainly after the re-ionization and their stellar mass is proportional to the mass at the time when the halo became a MW satellite. This model has 3 parameters (f_*, critical velocity and z_{reion}).

The third recipe is based on the Gnedin (2000) results, where we parametrize their characteristic mass by the characteristic critical velocity. To some extent this model is just smoother version of the previous recipe

$$M_* = \frac{f_* \times M_{DM}}{(1 + 0.26\,(V_{crit}/V_{circ})^3)^3}$$

After assigning the stellar masses to different sub-halos, we determine its detectability based on Koposov et al. 2007 result. Also for each dwarf galaxy in the simulations we solve the Jeans equation for the stellar body inside a NFW halo to determine the velocity dispersion of stars.

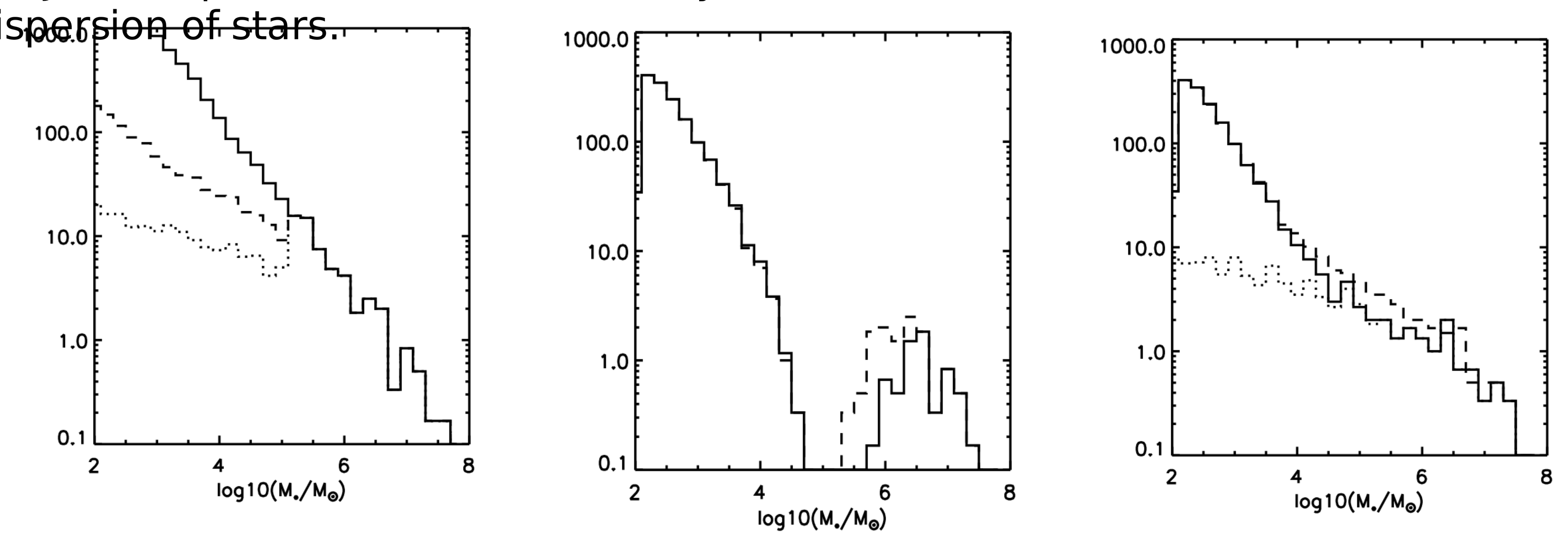

Fig 4: The distribution of stellar masses in the MW subhalos within the MW virial radius for different SF recipes. The left plot shows the distribution of stellar masses for the constant star formation efficiency and power-law star formation efficiency. The middle plot shows the mass distribution for the second SF recipe with sharp circular velocity threshold. The right plot shows the distribution of stellar masses for Gnedin(2000) model with different critical velocities.

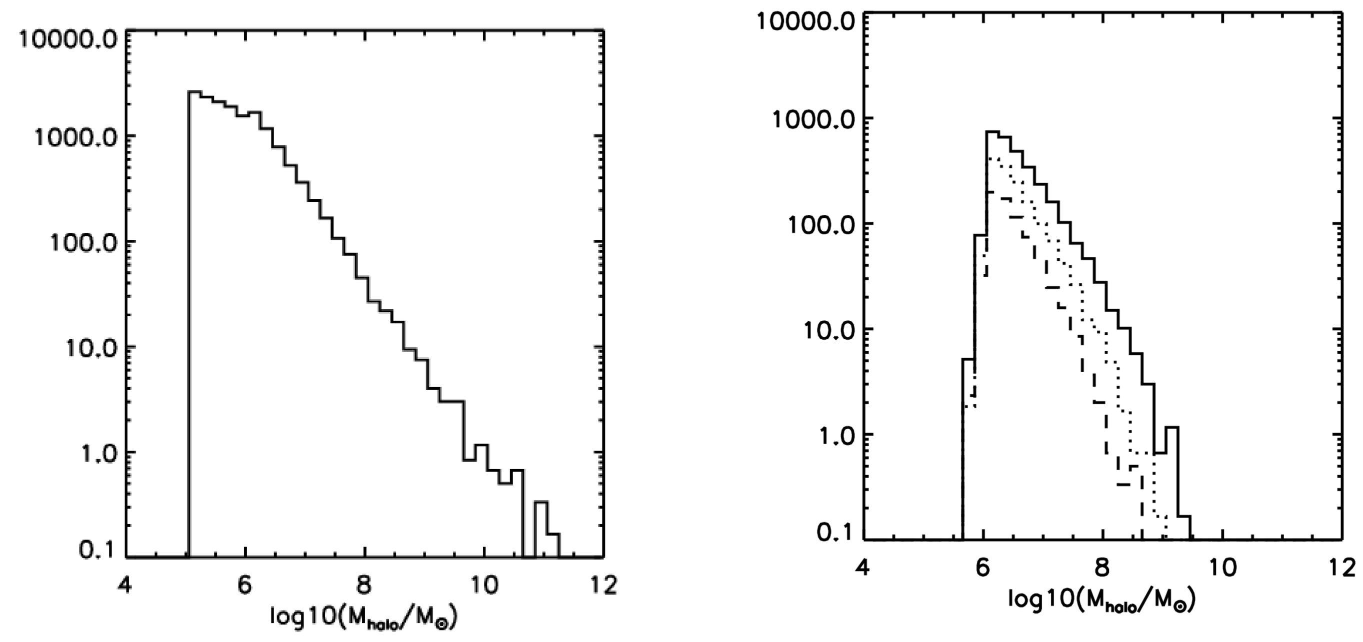

Fig1: The distribution of MW subhalo masses in our model at z=0 (left panel). The distribution of the halo masses of the present day MW subhalos at z=8,10, 12

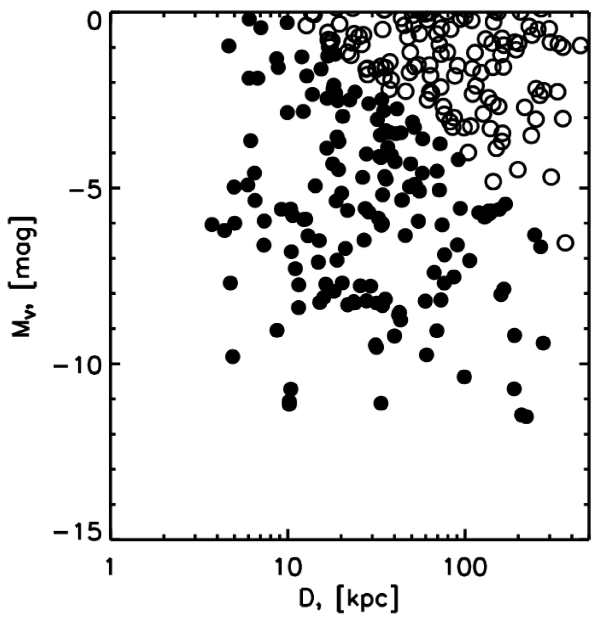

Fig. 2: Luminosity of dwarfs vs galactocentric distance in one of the simulations. Filled circles denote potentially detectable in SDSS galaxies, empty circles denote undetectable in SDSS galaxies according to Koposov et al. 2007 detectability criterion.

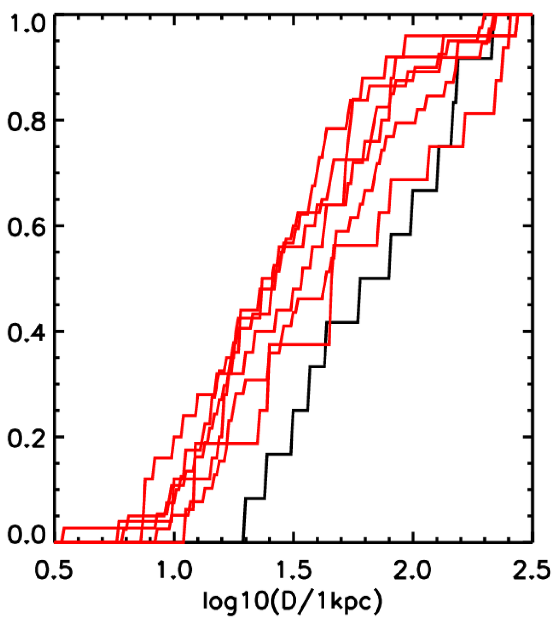

Fig 3: Cumulative distribution of heliocentric distances for the observed dwarfs (black line) and potentially observable dwarfs from 6 simulations (red line).

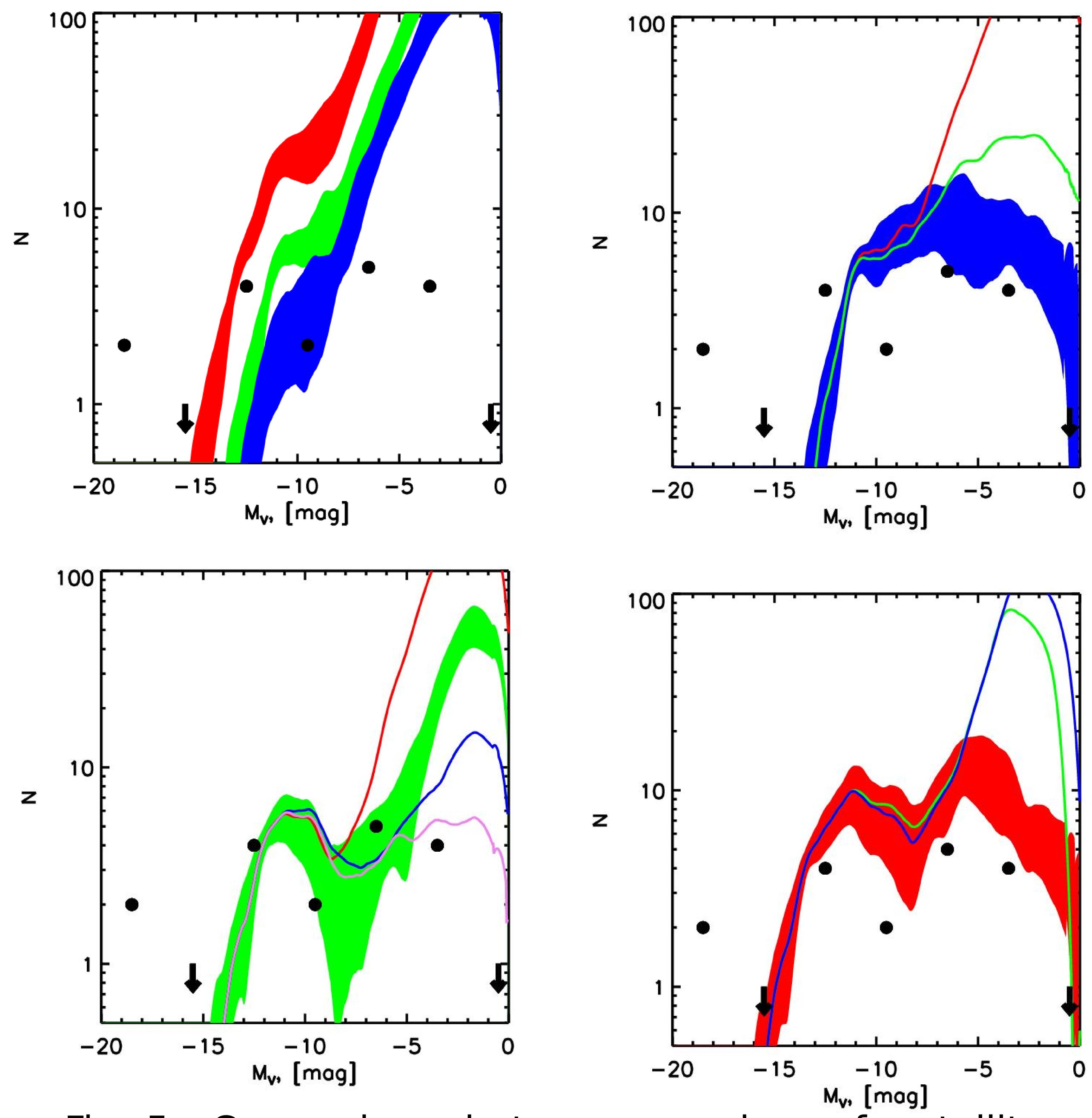

Fig 5: Comparison between number of satellites of different luminosities in the observations and simulations. The number of observed satellites is shown by filled circles and arrows (the binning with the bin size of 3mag was performed). The lines show the predictions of the models. For some models the filled area show the observed variance in different Monte-Carlo realizations.
The top left plot shows the number of satellites for the $M_*=f_* M_{DM}$ model with different f_*. The top right plot shows the number of satellites when f_* is a power-law of M_{DM} with different values of exponent. The bottom left plot shows the number of satellites for the Gnedin(2000) model with different re-ionization redshifts (z=8.10,15,30 – red,green, blue, pink). The bottom right panel shows the number of satellites for the Gnedin(2000) model with V_{crit}=35 km/s) and with different thresholds for pre-reionization star formation (10, 5, 0 km/s – red, green, blue)

Discussion and results

In Fig. 5 we compare the observed distribution of luminosities of dwarfs in the simulations and observations. The figure clearly shows that e.g. the M_* M_{DM} recipe clearly over-predicts the number of faint galaxies as it was expected. But the model with power-law $f_*(M_{DM})=f_{*,0}M^3$ may approximately reproduce the number of observed dwarfs (blue line on the top right panel of Fig 5).

The Gnedin(2000) model with reasonable values of critical velocities Vcrit=25-45 km/s may well reproduce the number of bright observed MW satellites. But it still overproduces the number of faint objects due to the significant pre-reionization star-formation (bottom left panel of Fig. 5). But if one takes into account that before the epoch of reionization only halos with V_{circ}>10km/s (Haiman 1997, Bovill&Ricotti 2008) were able to form stars, the number of faint galaxies come into much better agreement with the observations (see top right panel of Fig. 5).

Fig. 6 shows the luminosity and velocity dispersion distributions of the best fit Gnedin(2000) model. Combining that with Fig. 3, one can see, that the model is able to approximately reproduce the distribution of the main parameters of dwarfs (luminosity, distance, velocity dispersion). In that particular model, the galaxies in the bright end of the LF have formed their stars mostly after the epoch of re-ionization but the population of faint galaxies have formed significant amount of stellar mass before the re-ionization.

Conclusions

We have performed the semi-analytic simulation of the MW halo, populated all the MW sub-halo with stars by using simple semi-analytic recipes and measured the properties of the dwarf galaxies sitting in these halos. We have taken into account the incompleteness effects. The Gnedin(2000)-like recipe with characteristic velocity of V_{crit}=35 km/s, star formation efficiency of 10^{-2} allows us to obtain a reasonable agreement between the model and the observations in distributions of luminosities, distances and velocity dispersions of dwarf galaxies.

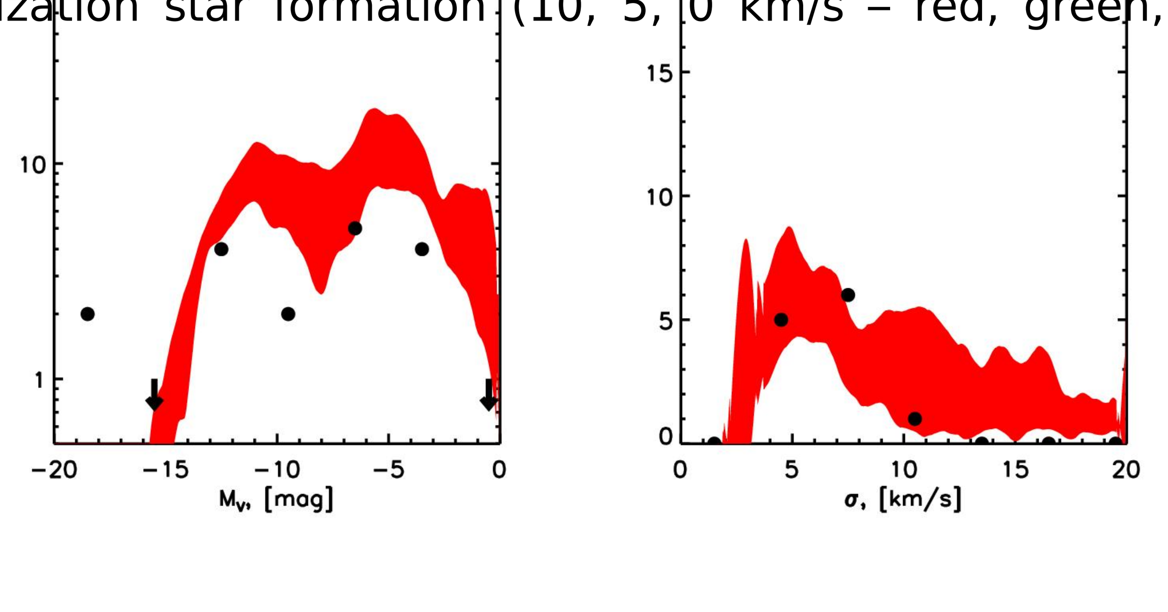

Fig. 6: The comparison of number of objects of different luminosities (left panel) and different velocity dispersions(right panel) for the observations (black circles and arrows) and Gnedin (2000) model with $f_*=10^{-2}\Omega_B/\Omega_M$, V_{crit}=35km/s, z_{reion}=11. Filled area shows the distributions for the model with 1σ contours showing the variance in different MC realizations